IBM Research Report

On Algebraic Smoothing: Theory and Results

S. Ghosal
IBM Research Division
IBM India Research Lab
Block I, I.I.T. Campus, Hauz Khas
New Delhi - 110016. India.

IBM Research Division
Almaden - Austin - Beijing - Delhi - Haifa - T.J. Watson - Tokyo - Zurich

Abstract

A Weighted Jacobi iteration based algebraic technique is proposed for smoothing discrete data, e.g., signal, image or video on grids with arbitrary topology. Energy of the discrete data is defined in H^1-space and a requirement for discrete scale-space theory is proposed based on the non-increase of energetic norm of the data. A shape-preserving smoothing method is also derived using a combination of Jacobi smoothers. Scale-selective smoothing of the data is achieved by eigenanalysis of the stiffness matrix. Experimental results are shown for isotropic image data.

1 Introduction

An inherent property of objects in the world and their representation in digital imagery is that they exist in certain ranges of scales. Since, elaborate procedure for finding relevant scales in the visual front-end may not be feasible for emerging active vision applications, multi-scale representation of images is recognized as a viable alternative. In fact multi-scale descriptions appeared in early days of computer vision. More recently, the scale-space presentation, introduced by Witkin [1] and Koenderink [2] provides a methodology for treating size or scale variations in the image data. The basic idea is to embed any measured data into a family of gradually smoothed and simplified data in which fine-scale information is suppressed. Traditionally the problem is formulated in 1-D in the continuous domain. Approximation in 2-D is obtained usually by taking Cartesian product of discrete 1-D kernels.

1-D continuous scale-space theory was first developed based on *causality* and *homogeneity* requirements. The observation that new local extrema cannot be created when increasing the scale parameter in the 1-D case shows that the Gaussian convolution satisfies certain sufficiency requirements for being a smoothing operation. The first proof of necessity of Gaussian smoothing for a scale-space representation was presented by Koenderink, who formally extended the scale-space theory to higher dimensions. He introduced the concept of *causality*, i.e., new level surfaces $\{(x, y; t)\} \in R^2 \times R : I(x, y; t) = I_0$ must not be created in the scale-space representation when the scale parameter t is increased. By combining causality which *isotropy* and *homogeneity*, which essentially mean that all spatial positions and all scale levels must be treated in a similar manner, it was shown that scale-space representation must satisfy the diffusion equation

$$\frac{\delta I}{\delta t} = I_{xx} + I_{yy}. \tag{1}$$

Given an initial heat distribution $I(.; 0) = I_0$, the diffusion equation governs the heat distribution I over time t in a homogeneous medium with uniform conductivity. Since the Gaussian kernel is the Green's function of the diffusion equation at an infinite domain, it follows that Gaussian kernel is the unique kernel for generation of the continuous scale-space. Lindeberg considered the scale-space description according to the requirement that scale-space kernels must not introduce new local extrema in a signal under convolution [3]. Such kernel can easily be shown to be positive and unimodal both in spatial and frequency domains. Interestingly, group-theoretic treatment of scale-space theory also uniquely leads to Gaussian scale-space kernel in continuous case. Despite the completeness of these results, however, they cannot be extended directly to 2-D and 3-D, even in continuous case.

Real-world signals/images obtained from standard digital cameras are discrete and an obvious problem is how to discretize the scale-space theory while still maintaining the scale-space properties. The requirement of non-creation of local extrema along with semi-group property leads uniquely to binomial convolution kernels $(\frac{t}{n} \quad 1 - \frac{2t}{n} \quad \frac{t}{n})^n$, which are of finite support. Despite the completeness of results, once again

they cannot be extended to higher dimensions. Further complications arise when we address non-uniform discretization, e.g., in foveal sensors with smaller sensing element at the center and larger ones near the periphery. This is also true for 1-D shapes, represented by an ordered set of nonuniformly distributed high-curvature points.

In spite of restrictive but elegant theoretical properties of Gaussian kernels, they are probably the most widely used smoothing kernel. But due to the same requirement, of non-creation of local extrema it suffers from serious drawbacks. It is well known that Gaussian smoothing causes shrinkage of the original data. In other words, an image recursively smoothed with a Gaussian eventually converges to a uniform gray [4]. Smoothing of a circle produces progressively smaller circles. This is because convolution with a Gaussian is not a low-pass operation – all but the zero frequency is attenuated [5] (strictly speaking, it is low-pass filter centered at zero frequency with zero bandwidth). To prevent shrinkage, the smoothing algorithm must produce a low-pass filtering effect with low-zero bandwidth. Oliensis proposed a Fourier descriptor based 1-D and 2-D smoothing technique that employs approximately reproducing kernels to prevent shrinkage. But this method too is valid for isotropic image lattices and does not extend to surfaces of arbitrary topological type. It is interesting to note that shape from deformation theory of Kimia *et al.*[6] extends to only limited topologies and also produces shrinkage. Recently Taubin proposed an weighted averaging based $O(n)$ technique for curve and surface smoothing without shrinkage and presents intuitive geometric validations. It is not clear how the weights are chosen when grid points are not equidistant. In this paper, I present a general theory for algebraic smoothing based on the energetic norm of the data, borrowing ideas from smoothing methods used in iterative solution of partial differential equations. Digitized data from real-world can be associated with H^1-space. The energy of the data is defined in H^1-space and a corresponding stiffness matrix is generated. The stiffness matrix is dependent on the topological connections on the sampling lattice and can be independent or dependent of the sensed data itself. Weighted Jacobi smoother based kernels are derived next based on eigenproperties of the stiffness matrix. These class of kernels ensure that energetic norm of the smoothed data does not increase w.r.t. the norm of the original data. This condition is valid in higher dimensions as long as the sampling topology belongs to the class of conforming finite elements, which probably covers all realistic sensor topologies. The entire smoothing technique is local and $O(n)$, and can be easily parallelized. In uniformly discretized 1-D case, it reduces approximately to the binomial kernels of Lindeberg [3]; in isotropic 2-D case, it is almost similar to Cartesian product of binomials. Some theoretical justifications are provided for simple cases, and experimental results are reported with a real isotropic 2-D image. The rest of the article is presented keeping the imaging community in mind – the theory and algorithms, however, can be directly applied to other discrete data, e.g, 1-D curves, 3-D surfaces, and spatiotemporal video.

2 Preliminaries

In this section I first present some notation and definitions related to this paper, and introduce the idea of energy functional of discrete data.

2.1 Notation

Some useful norms and inner products are defined in this subsection. On the vector space R^m, where m is positive integer, l^2 inner product and norms are defined as,

$$\langle x, y \rangle_{R^m} = \sum_{i=1}^{m} x_i y_i, \qquad || \ x \ ||_{R^m} = \langle x, x \rangle_{R^m}^{1/2}$$

Let Ω be the domain where the image is defined. We will recall definitions of L^2 inner product and norm, H^1 inner product, norm and semi-norm. In the following definitions, all functions x, and y are taken into account for which the corresponding integrals written below are defined. Derivatives are understood in distributive sense.

$$(x, y)_{L^2(\Omega)} = \int_\Omega xy d\Omega, \qquad || \ x \ ||_{L^2(\Omega)} = (x, x)_{L^2(\Omega)}^{1/2},$$

$$(x, y)_{H^1(\Omega)} = \int_\Omega \nabla x \dot{\nabla} y d\Omega, \qquad | \ x \ |_{H^1(\Omega)} = (x, x)_{H^1(\Omega)}^{1/2},$$

$$|| \ x \ ||_{H^1(\Omega)} = || \ x \ ||_{L^2(\Omega)} + | \ x \ |_{H^1(\Omega)} \ .$$

Finally, L^2 and H^1 spaces are defined as,

$$L^2(\Omega) = \{x : \quad || \ x \ ||_{L^2(\Omega)} < \infty\},$$

$$H^1(\Omega) = \{x : \quad | \ x \ |_{H^1(\Omega)} < \infty\}.$$

2.2 Energy of Image

Let us represent an $M \times N$ image in the lexicographic form as a vector $\hat{v} \in R^{n_1}$, where its i-th entry $\hat{v}_i$ is the intensity at i-th pixel. So, R^{n_1} can be understood as the space of all admissible images.

We construct a triangular mesh by connecting any image pixel to its N, E and NE neighbors. We define the standard P^1-finite element (FE) space $V_1 \subset H^1(\Omega)$,

$$V_1 = span\{\phi_i^1\}_{i=1}^{n_1}.$$

The basis function ϕ_i^1 is a continuous function, linear at each triangle, and satisfying

$$\phi_i^1(x_j, y_j) = \begin{cases} 1 & \text{iff } j = i \\ 0 & \text{otherwise} \end{cases}$$

where $(x_i, y_i)^T$ denote the coordinates of the i-th pixel. The interpolation operator, $\Pi_1 : R^{n_1} \to V_h$ is defined in the usual way,

$$\Pi_1 \hat{v} = \sum_{i=1}^{n_1} \hat{v}_i \phi_i^1. \tag{2}$$

The representation of the function $v \in V_h$ w.r.t. the basis $\{\phi_i^1\}_{i=1}^{n_1}$ is denoted by $\hat{v}$, i.e.,

$$v = \Pi_1 \hat{v}.$$

Let us define *relative energy* of the image as,

$$E(v) = \frac{| \ v \ |_{H^1(\Omega)}^2}{|| \ v \ ||_{L^2(\Omega)}^2}. \tag{3}$$

The numerator attains a high value for strong spatial variation of intensities in an image. The L^2 norm in the denominator assures the *scaling invariance*, i.e.,

$$E(tv) = E(v)$$

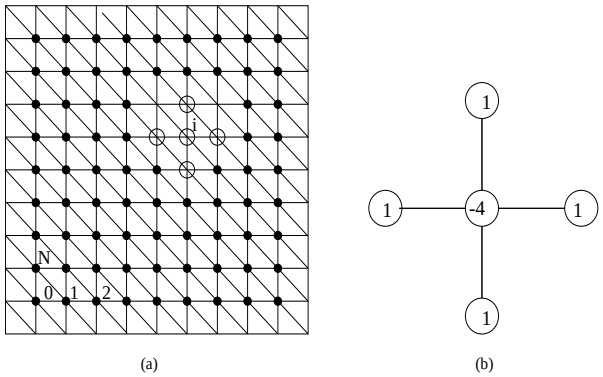

Figure 1: Finite-element discretization of isotropic image domain. (a) The finite-element grid corresponding to 5-point finite-difference scheme. (b) The 5-point stencil.

where $t \in R$. The numerator can be rewritten as,

$$| v |^2_{H^1(\Omega)} = | \Pi_1 \hat{v} |^2_{H^1(\Omega)} = \langle A^1 \hat{v}, \hat{v} \rangle_{R^{n_1}} \tag{4}$$

where, $A^1 = \{a^1_{ij}\}^{n_1}_{i,j=1}$ is the so-called *stiffness matrix*, with entries $a_{ij} = (\phi^1_i, \phi^1_j)_{H^1(\Omega)}$, and denominator as,

$$|| v ||^2_{L^2(\Omega)} = || \Pi_1 \hat{v} ||^2_{L^2(\Omega)} = \langle M^1 \hat{v}, \hat{v} \rangle_{R^{n_1}} \tag{5}$$

where, $M^1 = \{m^1_{ij}\}^{n_1}_{i,j=1}$ is the so-called *mass matrix* with entries $m_{ij} = (\phi^1_i, \phi^1_j)_{L^2(\Omega)}$. Thus,

$$E(v) = \frac{\langle A^1 \hat{v}, \hat{v} \rangle_{R^{n_1}}}{\langle M^1 \hat{v}, \hat{v} \rangle_{R^{n_1}}}. \tag{6}$$

For the five-point finite-difference discretization shown in Fig. 1(a) for a uniform image grid, the stiffness matrix A^1 is symmetric, and positive semi-definite with a stencil corresponding to the 5-point scheme, given in Fig. 1(b). Further from Fig. 1, $a_{ii} = 4$ for interior pixel i, $a_{ii} = 3$ for noncorner boundary pixel i, and $a_{ii} = 2$ for corner pixel i. $a_{ij} = -1$ if pixels i and j are *four-connected* neighbors. a_{ij}'s are zero otherwise.

For computing $E(\hat{v})$ approximately, construction of mass matrix M^1 is not necessary. It is well known [7] that mass matrix M^1 is spectrally equivalent to $h^2 I$, where h is the discretization, and consequently we have the following scaled equivalence of continuous L^2 and discrete l^2 norms,

$$c \, || \Pi_h \hat{v} ||_{L^2(\Omega)} \leq h^2 \, || \hat{v} ||_{R^{n_1}} \leq C \, || \Pi_h \hat{v} ||_{L^2(\Omega)} \, . \tag{7}$$

where, c and C are constants independent of mesh-size.

The energy is related to the Fourier representation of images in frequency domain. Eigenvectors of the matrix A^1 are of the form $sin(\omega_x x_i) sin(\omega_y y_i)$ for certain frequencies (ω_x, ω_y). The corresponding eigenvalues are increasing with increasing (ω_x, ω_y). Taking into account (6) and (7), the energy of eigenvectors tends to increase with increasing frequencies (ω_x, ω_y).

3 Weighted Jacobi Smoother

A simple technique for smoothing of discrete data is presented here, borrowing ideas from the theory of iterative solution techniques for elliptic partial differential equations [9]. Let X be the discrete data vector, and A be the stiffness matrix is created

as shown in Fig.1 by associating the finite element grid with the sampling topology. Then, the smoothing of data can be expressed as

$$X^{t+1} = S_l X^t = \left(I - \omega D^{-1} A\right) X^t \tag{8}$$

where X^{t+1} is the data vector at time $(t+1)$, D is the diagonal matrix consisting of diagonal elements of A, I is an identity matrix with size equal to the size of the dataset, N, and ω is known as the damping weight. Since the data vector X belongs to the H^1-space, its energetic norm can be defined as,

$$E(X) = \langle AX, X \rangle \tag{9}$$

In the case of uniform discretization in 1-D, (9) reduces to,

$$E(X) = \sum_{i=0}^{N} x_i(2x_i - x_{i+1} - x_{i-1})$$

which is closely related to number of extrema as discussed in [3]. We propose that for discrete data in arbitrary dimension and with arbitrary topology, *scale-space kernels be designed in a way that the energetic norm of the data does not increase with the amount of smoothing*, i.e.,

$$\langle AX^{t+1}, X^{t+1} \rangle \leq \langle AX^t, X^t \rangle. \tag{10}$$

We prove that the choice of Jacobi smoother satisfies the requirement of non-increase of energetic norm for 1-D or 2-D regular mesh. Similar proofs can be obtained following the concept of weighted Sobolev space for irregular meshes [8]:

$$\begin{aligned} \langle AX^{t+1}, X^{t+1} \rangle &= \langle AS_l X^t, S_l X^t \rangle = S_l^2 \langle AX^t, X^t \rangle \\ &\leq \lambda_{max}(S_l^2) \langle AX^t, X^t \rangle \end{aligned} \tag{11}$$

where, $\lambda_{max}(S_l)$ is the spectral radius of matrix S_l, or in other words largest eigenvalue. If the problem domain is 1-D uniform, then eigenvalues of A are

$$\lambda(A) = 4sin^2\left(\frac{m\pi}{2N_x}\right), m = 1, .., N_x.$$

If the problem domain is the 2-D isotropic image,

$$\lambda(A) = 4sin^2\left(\frac{m\pi}{2N_x}\right) + 4sin^2\left(\frac{n\pi}{2N_y}\right)$$

Clearly, for 1-D and 2-D uniform discretizations,

$$\langle AX^{t+1}, X^{t+1} \rangle \leq (1 - 2\omega)^2 \langle AX^t, X^t \rangle$$

For convergence,

$$-1 \geq \lambda_{max}(S_l) \leq 1$$

$$\text{or,} \quad -1 \leq 1 - 2\omega \leq 1 \tag{12}$$

$$\text{or,} \quad 0 \leq \omega \leq 1 \tag{13}$$

Since $sin^2\left(\frac{t\pi}{2}\right) > 0$ for all nonzero t, $\lambda(S_l) < 1$ for all nonzero t. On in other word, energy associated with all eigenvectors decreases – of course, high-frequencies are attenuated faster than low-frequency one. As a consequence, shrinkage occurs for all shapes with succesive application of the smoother. Higher the value of ω, the lower

are the eigenvalues, resulting in greater smoothing. The value of ω that provides the optimal damping of the oscillatory components, i.e., scale > 0.5 can be obtained by requiring [9],

$$\lambda_{\frac{N_x}{2}}(S_l) = -\lambda_N(S_l).$$

Interestingly, the solution $\omega = \frac{2}{3}$ has been empirically found to be optimal for generating Laplacian pyramid.

3.1 Adaptive Smoothing

Here I discuss the properties of multiple Jacobi smoothers of the form

$$S_l = (I - \omega_1 D^{-1}A)(I - \omega_2 D^{-1}A),$$

and present the necessary conditions for convergence and adaptive smoothing. As before, for convergence,

$$-1 \leq \lambda_{max}(S_l) \leq 1 \tag{14}$$

It is easy to obtain,

$$\lambda(S_l) = 1 - 2(\omega_1 + \omega_2)\sin^2\left(\frac{t\pi}{2}\right) + 4\omega_1\omega_2\sin^4\left(\frac{t\pi}{2}\right). \tag{15}$$

Both $\omega_1 < 0$, and $\omega_2 < 0$ leads to instability, since for $t > 0$, $\lambda(S_l) > 1$. Smoothing with $\omega_1, \omega_2 \geq 0$ is simply equivalent to two single Jacobi smoothers with ω_1 and ω_2. Thus, $0 \leq \omega_1, \omega_2 \leq 1$ ensures convergence for $\omega_1, \omega_2 \geq 0$. If $\omega_1 = -\delta_1, \omega_2 = -\delta_2 \leq 0$,

$$\begin{aligned} \lambda(S_l) &= 1 - 2(\omega_1 + \omega_2)\sin^2\left(\frac{t\pi}{2}\right) + 4\omega_1\omega_2\sin^4\left(\frac{t\pi}{2}\right) \\ &= 1 + 2(\delta_1 + \delta_2)\sin^2\left(\frac{t\pi}{2}\right) + 4\delta_1\delta_2\sin^4\left(\frac{t\pi}{2}\right) > 1. \end{aligned} \tag{16}$$

Hence, both $\omega_1 < 0$, and $\omega_2 < 0$ leads to instability.

Let us now analyze the interesting behavior of the multiple Jacobi smoothers with $\omega_1\omega_2 < 0$. Substituting $X = \sin^2\left(\frac{t\pi}{2}\right) \geq 0$, we get

$$\lambda(S_l, X) = 1 - 2(\omega_1 + \omega_2)X + 4\omega_1\omega_2X^2. \tag{17}$$

Differentiating Equation 17 w.r.t. X and equating to zero, we obtain

$$\lambda_{max}(S_l, X) = 1 - \frac{(\omega_1 + \omega_2)^2}{4\omega_1\omega_2}, \tag{18}$$

for $\omega_1 + \omega_2 \leq 0$. $\omega_1 = -\omega_2$ ensures asymptotic convergence. If $\omega_1\omega_2 < 0$, and $\omega_1 + \omega_2 > 0$, asymptotic convergence is guaranteed if

$$\begin{aligned} \lambda_{max}(S_l, X) &= 1 - 2(\omega_1 + \omega_2)X_{max} + 4\omega_1\omega_2X_{max}^2 \geq -1 \\ \text{or, } \omega_2 &\leq \frac{1 - \omega_1}{1 - 2\omega_2} \end{aligned} \tag{19}$$

The frequency characteristics of $\lambda(S_l)$ for multiple Jacobi smoothers are shown in Figures 2, 3, and 4, respectively, for $\omega_1 = 0.5$, $\omega_1 = 0.7$, and $\omega_1 = 1.0$. The low-frequency and high-frequency behaviors for $\omega_1 = -\omega_2$ are shown in detail in Figures 5, and 6, respectively. Clearly, if $\omega_1 = -\omega_2$, $\frac{\delta\lambda(S_l)}{\delta k} \approx 0$ near zero frequency. Thus, recursive filtering does not cause the shrinkage of shapes of moderate size. However, the high-frequency behavior of the smoother depends on the value of ω_1. Substituting

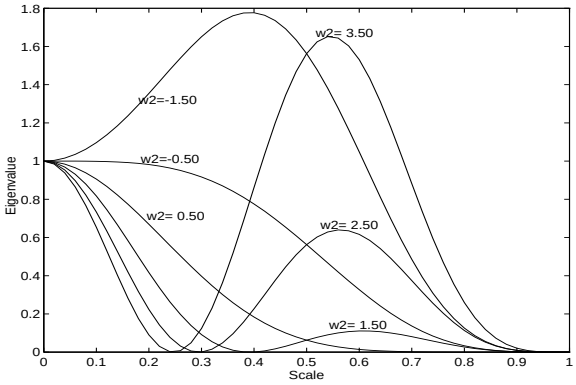

Figure 2: Eigenvalues of multiple Jacobi smoother for $\omega_1 = 0.5$.

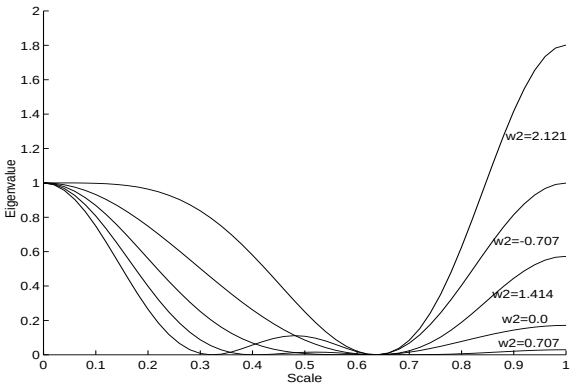

Figure 3: Eigenvalues of multiple Jacobi smoother for $\omega_1 = 0.70$.

$\omega_1 = -\omega_2 = \omega$, and $X = 1$ corresponding to pure high-frequency in Equation 17, we obtain,

$$\lambda(S_l, 1) = 1 - 4\omega^2. \tag{20}$$

Thus, simultaneous high-frequency (e.g., noise) attenueation and shape preservation can be achieved, if $\omega = 0.5$. Other desired frequency characteristics can be obtained in a similar manner.

Convergence is not guatanteed if $\omega_1 + \omega_2 < 0$, as proved above, and as evident from $|\lambda_{max}(S_l)| > 1$ in the Figures. For certain choices of of ω_1 and ω_2, it can be seen that certain frequencies are actually enhanced. For these choices, asymptotic convergence is not possible, but useful enhancement can be obtainedby applying the smoother combination for a few times.

Note that the above closed-form results are obtained for uniformly sampled discrete 1-D signals and 2-D image data. Similar results can be obtained for other discrete data sequences of arbitrary dimension from the corresponding finite-element discretizations.

4 Results

Figure 7(a) shows a 128×128 images, taken from the MIT Vistex database. Uniform noise with zero mean and standard deviation 100 is added to obtain a signal-to-noise ratio of approximately 12 dB w.r.t. the original image. This noisy version of the original is shown Figure 7(b). The result obtained by recursively applying a single Jacobi smoother with $\omega = 0.67$ for 300 iterations is described in Figure 7(c). Clearly, all the structures in the original image have collapsed. The signal-to-noise

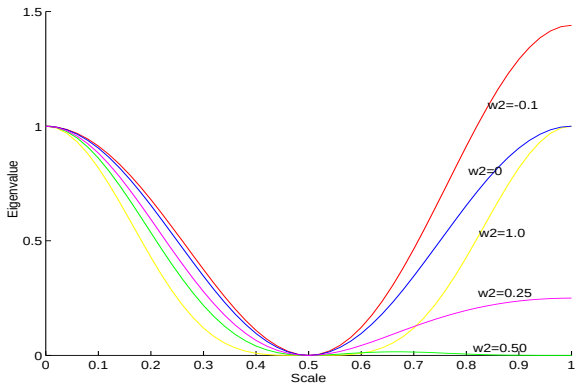

Figure 4: Eigenvalues of multiple Jacobi smoother for $\omega_1 = 1.0$.

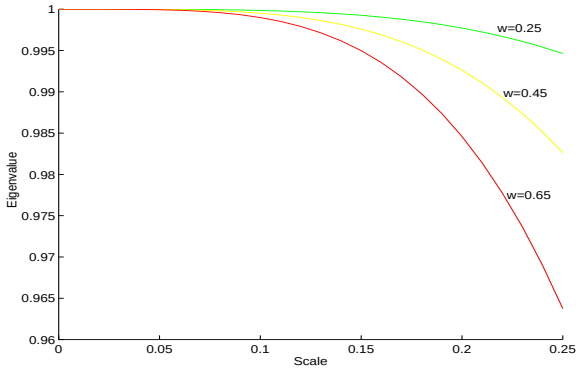

Figure 5: Low-frequency characteristics of eigenvalues for $\omega_1 = -\omega_2$.

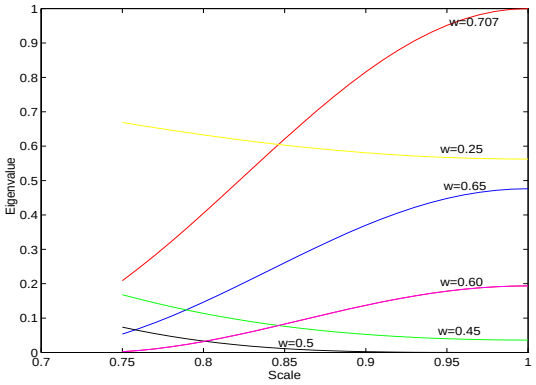

Figure 6: High-frequency characteristics of eigenvalues for $\omega_1 = -\omega_2$.

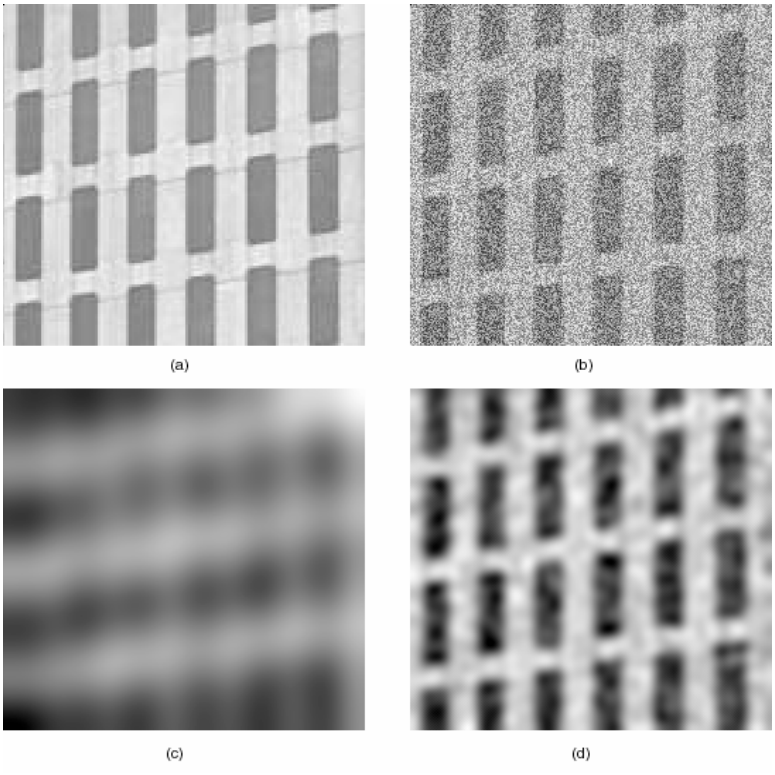

Figure 7: Simultaneous noise cleaning and shape preservation. (a) Original image. (b) Original image plus uniform noise. (c) Asymptotic Gaussian smoothing. (d) Asymptotic multiple Jacobi smoothing with $\omega_1 = -\omega_2 = 0.5$

ratio w.r.t. the original image is only 18 dB. Recall that a single Jacobi smoother with $\omega = 0.67$ is same as the well-known discrete Gaussian smoother. Figure 7(d) deonstrates the shape-preserving noise cleaning behavior of the combination of Jacobi smoothers with $\omega_1 = -\omega_2 = 0.5$. The smoothers have been applied for 300 iterations, just like in Figure 7(c).

These and other results establish the usefulness of Jacobi smoothers in adaptive smoothing of discrete data.

5 Conclusions

Here I propose a novel methodology for algebraic smoothing of discrete data based on the eigenvalue analysis of stiffness matrices. The energy of the discrete data is defined in H^1-space, and a discrete scale-space theory is developed based on non-increase of energetic norm of the data. A combination of two Jacobi smoothers is analyzed for uniformly sampled 1-D and 2-D data, and parameters are determined for ensuring asymptotic convergence, shape preservation, noise cleaning, and selective enhancement. The proposed technique is valid for arbitrary dimensions, as long as the sampling topology belongs to the class of conforming finite-elements, which probably covers all realistic data acquisition scenarios, including 1-D curves, 3-D surfaces, spatio-temporal video. The proposed technique can be easily applied to visualization of complex scientific data, and registration of multimodal medical data. We are currently working on the application of the proposed method for shape modification of a query object. Learning of user perception through modification of a query object is very useful in a perceptual and user-friendly image retrieval system [10].

References

[1] A.P. Witkin, "Scale space filtering," *Proc. IJCAI*, pp. 1019–1023, Karlsruhe, Germany, 1983.

[2] J.J. Koenderink, "The structure of images," *Biological Cybernetics* vol. 50, pp. 363–370, 1984.

[3] T. Lindeberg, B.M. ter Haar Romeny, "Linear scale-space I: Basic Theory," in *Geometry-Driven Diffusion in Computer Vision*, Haar Romeny (ed.), pp. 1–37, Kluwer Academic, 1994.

[4] J. Oliensis, "Local reproducing smoothing without shrinkage," *IEEE Trans. PAMI*, vol. 15, no. 3, pp. 307–312, 1993.

[5] G. Taubin, "Curve and surface smoothing without shrinkage," *Proc. ICCV*, Cambridge, 1995.

[6] B.B. Kimia, K. Siddiqi, "Geometric heat equation and nonlinear diffusion of shapes and images," *Proc. CVPR*, pp. 113–120, Seattle, 1994.

[7] C. Johnson, *Numerical Solution of Partial Differential Equations By The Finite Element Method*, Cambridge Univ. Press, 1987.

[8] P. Vanek et al., *Algebraic Multigrid On Unstructured Meshes*, Report no. 34, Center for computational math, Univ. of Colorado at Denver, 1995.

[9] W.L. Briggs, *A Multigrid Tutorial*, SIAM, Philadelphia, 1987.

[10] G. Aggarwal, P. Dubey, S. Ghosal, A. Kulshreshtha, A. Sarkar, "iPURE: Perceptual and User-friendly REtrieval of Images," Proc. IEEE Conf. on Multimedia and Expo, New York, 2000, to appear.